Active tectonic analysis of Atrak river subbasin located in NE Iran (East Alborz)

Maryam Ezati[1],* Maryam Agh–Atabai[2]

1- M. Sc. Department of Geology, Faculty of Sciences, Golestan University, Gorgan, Iran.
2- Assistant Professor, Department of Geology, Faculty of Sciences, Golestan University, Gorgan, Iran.

* Corresponding Author: Geology1200@yahoo.com

Received: 28 August 2013 / Accepted: 14 October 2013 / Published online: 20 October 2013

Abstract

Study of tectonic affects in many fluvial systems shows that, rivers are valuable tools to active tectonics surveying. Study of stream channels and their associated deposits offset by faulting may reveal the amount displacement at particular site and give information that is critical for future earthquake hazards evaluation. Study area which is a subbasin of Atrak river is located at the NE Iran (East Alborz) and west of Bojnurd city. Aim of this research is separating high tectonic activity areas from low tectonic activity areas. In this research, in order to evaluate rate of tectonic activity the drainage basin asymmetry factor (*Af*), Transverse topographic symmetry factor (*T*), hypsometric integral (*Hi*) hypsometric curve (Hc), stream–gradient index (*SL*), valley floor width–valley height ratio (*Vf*) and Relative tectonic activity (*Iat*) were calculated. Based on Iat values, the study area was divided into four parts: Class 1 (very high relative tectonic activity: subbasin 2 and 3), class 2 (high relative tectonic activity: subbasin 4), class 3 (moderate relative tectonic activity: subbasin 5), class 4 (low relative tectonic activity: subbasin 1). Results of this research show that northern side of Qharajeh basin is inactive part of study area and southern side of Qharajeh basin is actives part.

Keywords: Active Tectonic, Atrak River, Geomorphic Index, East Alborz.

1– Introduction

Iran lies on the Alpine earthquake Belt which runs west–east from the Mediterranean to Asia. The present tectonics of Iran results from the north–south convergence between the plates of Arabia to the southwest and Eurasia to the northeast (Jackson and McKenzie, 1984). This convergence is accommodated across the Iranian Plateau and adjacent deformed zones, and the deformation, as defined by seismicity, tectonic geomorphology, and geology is not uniformly distributed. Much of the deformation is concentrated in the Zagros active thin–skinned Fold and Thrust Belt in the southwest, Alborz Thrust Belt bordering oceanic crust of the south Caspian depression, Kopeh–Dagh active thin–skinned Fold Belt in the north east, and in East–Central Iranian thick–skinned range and basin province. The East Alborz, which is the subject of this paper, shortening across the East Alborz (Binalud) mountain range east of 57° E, is on major active thrust lineaments which bound the south side of the range and minor strike slip faults on the north side. Basin ward migration of faulting has resulted in a series of sub–parallel thrust faults along the range front. Now shortening is concentrated on the southernmost and youngest of these faults, which uplift Neogene deposits, forming a low step along the edge of the topography (Hollingsworth, 2007).

Rivers are very sensitive to any kind of change and tectonic control upon forms of rivers and streams in recent years. With recognition of tectonic effect in many fluvial systems recognized that rivers present a valuable tool for studies of active tectonics. The role of tectonics and active tectonics in morphological evolution of drainage basins is well reflected by the morphotectonic parameters of that basin. Study of stream channels and their associated deposits offset by faulting may reveal the amount displacement and timing of the last few earthquakes at particular site information that is critical in evaluating future earthquake hazards (Keller and Pinter, 2002). The objective of this paper is to identify the representative morphotectonic parameters that indicate the ongoing active tectonic activities in the area.

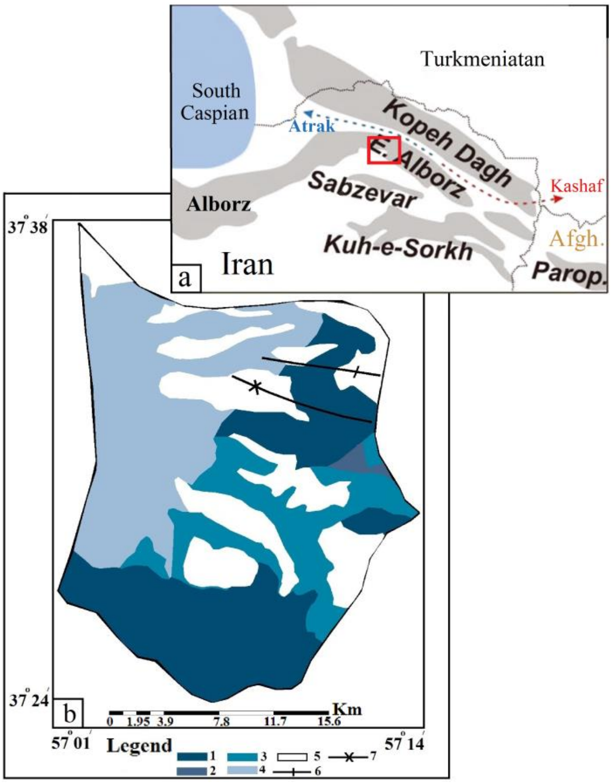

Figure 1) Locations map of the study area (Hollingsworth et al., 2010), (a); geological map of the study area (b); 1: Limestone with orbitolina (Tiregan Formation), 2: marl with orbitolina (Sarcheshmeh Formation), 3: shale and marl (Sanganeh Formation), 4: sandstone and shale (Aitamir Formation), 5: alluvial deposits, 6: Anticline 7: Syncline.

This article applies a quantitative geomorphologic method to an area in the East Alborz. We analyzed five geomorphic indices such as: drainage basin asymmetry factor (Af), Transverse topographic symmetry factor (T), hypsometric curve (Hc), hypsometric integral (Hi), the stream–gradient index (SL), valley floor width–valley height ratio (Vf). This kind of methodology has been found to be useful in various tectonically active areas such as: Contemporary uplift and erosion of the southern Alps (Adams, 1980), Neotectonics of North America (Slemmons et al., 1991), Golf of Corinth of Greece, (Verrior and Zygouri, 2004), northern Sicily, (Arisco and Arnone, 2006), the southwestern Sierra Nevada of Spain (El Hamdouni et al., 2008), Neotectonic East Sudeten Mountains (Czech Republic) (Stepancikova et al., 2008), Drainage network geometry versus tectonics in the Argentera Massif (French–Italian Alps) (Ribolini and Spagnolo, 2008), relative tectonic activity of Sarvestan area, central Zagros, Iran (Dehbozorgi et al., 2010), Active Tectonics of the South Central Alborz (North Iran) (Khavari et al., 2010).

2– Regional geology

The study area (328.56 km^2) is a subbasin of Atrak river is located at the East Alborz and west of Bojnurd city (Fig. 1a). To the north, the East Alborz is separated from the Kopeh Dagh by the major Atrak– Kashaf river valley. Litology map of study area shows that study area (Qharajeh basin) is composed of limestone with orbitolina (Tiregan Formation), marl with orbitolina (Sarcheshmeh Formation), shale and marl (Sanganeh Formation), sandstone and shale (Aitamir Formation), alluvial deposits (Fig. 1b). Digital elevation model (DEM) of Qharajeh basin shows that, highest elevation is related to southern side of study area and lowest elevation is associated with northern side of study area (Fig. 2).

The East Alborz–Binalud mountains lie parallel to the Kopeh Dagh of NE Iran. They comprise a region of predominantly Jurassic marine deposits, which structurally belong to Central Iran, contrasting with the Eurasian rocks of the

Kopeh Dagh. Geologically, they are a continuation of the main Alborz range, which borders the southern margin of the Caspian Sea (Alavi, 1996). The Binalud refers to a small section of the East Alborz, north of Neyshabur, in which metamorphosed Paleozoic rocks are exposed. Therefore, the Atrak–Kashafrud valley, which separates the Alborz and Kopeh Dagh, forms a major structural boundary between Central Iran and Eurasia, known as the Paleo–Tethys suture (Stocklin, 1968, 1974; Berberian and King, 1981; Alavi, 1991, 1996), which formed at the start of the Alpine–Himalayan orogeny.

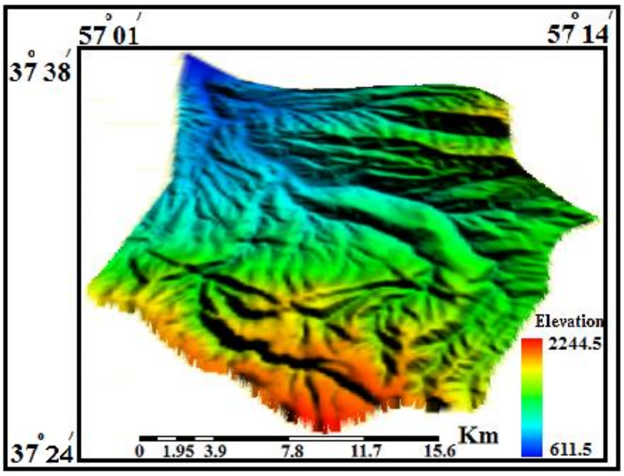

Figure 2) 3D digital elevation model (DEM) of study area.

The two ranges are comparable in size, with the highest peaks in the Binalud (3,000 m) occurring directly south of the highest peaks of the Kopeh Dagh (3,000 m), near 59°E. In NE Iran, the tectonics of the East Alborz range change significantly east and west of 57°E, and are probably related to a long– strike elongation occurring in the Central Kopeh Dagh to the north. This research examines the active tectonics of the East Alborz–Binalud east of 57°E, where NE–SW shortening occurs on major thrust faults on the south side of the range, which continues southeast into Afghanistan. Deformation north of the range is limited to minor left–lateral strike–slip north of Esfarayen, which may also be related to elongation in the Central Kopeh Dagh (Hollingsworth, 2007).

3– Materials and Methods

Lineament of study area are extracted from VNIR band of Aster image; with utilize 0◦, 45°, 90◦, 180° filters and from satellite image using visual interpretation.

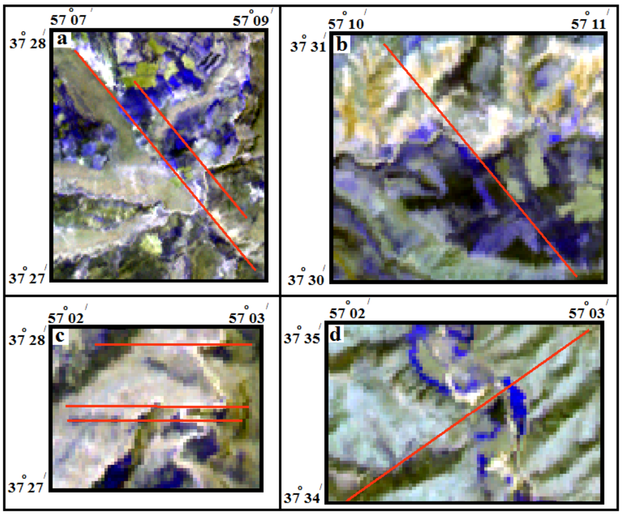

Figure 3) Aster image VNIR band of study areas from rivers offset. a) River deflected by lineament with NW–SE trending. b) by lineament with NW–SE trending. c) by lineament with E–W trending. d) by lineament with NE–SW trending.

The lineaments usually appear as straight lines or edges on the satellite images. Some general features that used for identifying lineaments in this research are: offset of rivers (Fig. 3), topographic features such as straight valleys, continuous scarps and straight rock boundaries.

Figure 4) Fault in Gorgan– Bojnurd road with E– W trending.

In this research field survey was done, for accuracy determination of extracted lineaments from the Aster image (Fig. 4). Interpretation of extracted lineaments from Aster image in rose diagram shows that most of lineaments of Qharajeh basin have NE–SW trending (Fig. 5).

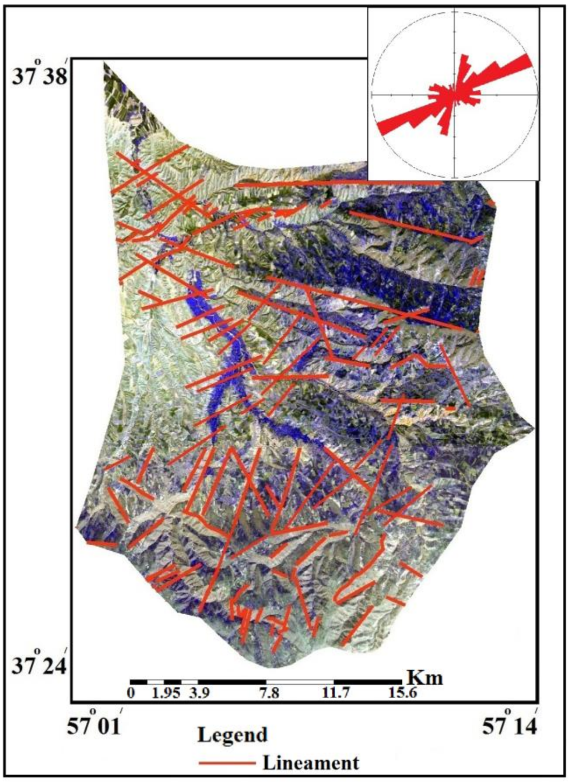

Figure 5) Lineaments extracted from aster image VNIR band, and rose diagram of lineaments.

Geomorphic indices developed as a tool to recognize areas experiencing rapid tectonic activity. In this study in order to evaluate rate of tectonic activity geomorphic indices drainage basin asymmetry factor (Af), transverse topographic symmetry factor (T), hypsometric curve (Hc), hypsometric integral (Hi), stream–gradient index (SL), valley floor width–valley height ratio (Vf), relative tectonic activity (Iat) were calculated.

3–1– Drainage basin asymmetry factor (*Af*):

The asymmetry Factor (Af) is defined as:

$$Af = 100\ (Ar/At) \quad (1)$$

Where *Ar* is the area of the basin to the right (facing downstream) of the main stream and *At* is the total area of the drainage basin. For a stream network that formed in a stable environment Value of *Af* index should be equal about 50. *Af* index is sensitive to tilting vertical to the trend of the trunk stream. Value of *Af* greater or less than 50 suggests that our study area is tilt (Keller and Pinter, 1996). The values were classified into three categories: 1 ($|Af–50|>15$), 2 ($|Af–50| = 7–15$), 3($|Af–50| < 7$) (El Hamdouni, et al., 2008).

3–2– Transverse topographic symmetry factor (*T*):

$$T = Da/Dd \quad (2)$$

Where *Da* is the distance from the midline of the drainage basin to the midline of the active meander belt, and *Dd* is the distance from the basin midline to the basin divide. For a perfectly symmetric basin, *T* = 0. As asymmetry increases, T increases and approaches a value of 1. Assuming that the dip of the bedrock can be shown to have insignificant influence on the migration of the stream channels then the direction of regional migration is an indication of the ground tilting in that direction (Cox, 1994). Thus, *T* is a vector with a bearing (direction) and magnitude from 0 to 1. *T* index can detect areas of lateral tilting (Cox, 2001).

3–3– Hypsometric integral (Hi):

The index is defined as the relative area below the hypsometric curve and thus expresses the volume of a basin that has not been eroded. The hypsometric integral (*Hi*) is defined as:

Mean elevation– minimum elevation / maximum elevation– minimum elevation (3)

Three values of the hypsometric integral easily earns from a topographic map. Maximum and minimum elevations are read immediately from topographic map. Mean elevation is obtained by point sampling of at least 50 values of elevation in the basin and calculating the mean (Pike et al., 1971), or by using digital elevation models (DEM). High values of the hypsometric integral show that most of the topographic is high associated with the mean, such as a smooth upland surface cut by deeply digging streams. Mediate to low values of hypsometric integral are related to more evenly digging drainage basin (Keller and Pinter, 1996). Values of *Hi* index were classified into three categories: 1 (Hi = 0.55–1), 2 (Hi = 0.45–0.55), 3(Hi = 0–0.45) (El Hamdouni et al., 2008).

3–4– Stream length– gradient (*SL*) index:

The stream length– gradient index is defined as:

$$SL = (\Delta H/\Delta L)L \qquad (4)$$

SL is the stream length–gradient (*SL*) index, $\Delta H/\Delta L$ is the channel slope or gradient of the reach (ΔH is the change in elevation of the reach and ΔL is the length of the reach) and L is the total channel length from the midpoint of the reach of interest upstream to the highest point on the channel (Keller and Pinter, 1996). This index is sensitive to change in gradient (Hack, 1973). Good correlation exists between rock resistance and stream length– gradient index. The SL index is used to recognize recent tectonic activity by identifying irregularly high index values on a particular rock type (Keller and Pinter, 1996). The values of *SL* index were classified into three categories: 1 ($SL \geq 500$), 2 ($300 \leq SL < 500$), 3($SL < 300$) (El Hamdouni et al., 2008).

3–5– Ratio of valley floor width to valley height:

The ratio of valley floor width to valley height (*Vf*) may be expressed as:

$$Vf = 2\, Vfw / [(Eld - Esc) + (Erd - Esc)] \qquad (5)$$

Where *Vf* is the valley floor width–to– height ratio; *Vfw* is the width of the valley floor; *Eld* is elevation of the left valley, *Erd* is elevation right valley and Esc is the elevation of the valley floor (Bull, 1977). This index difference between *U* shape valley with relatively high *Vf* values and *V* shaped valley with relatively low *Vf* values (Keller and Pinter, 1996). The values of *Vf* index were classified into three categories: 1($Vf < 0.5$), 2 (Vf 0.5–1), 3($Vf > 1$) (El Hamdouni et al., 2008).

3–6– Relative tectonic activity (*Iat*):

Several index combined to provide information of relative degree of tectonic activity. To provide *Iat* index is obtained by averaging of different classes of geomorphic indices (S/n) and divided in to four classes. Class 1 is very high tectonic activity with values of S/n between 1 and 1.5; class 2 is high tectonic activity with values of 2>S/n>1.5; class 3 is moderately active tectonics with 2.5>S/n >2; and class 4 is low active tectonics with values of S/n>2.5 (El Hamdouni et al., 2008).

4– Result and Discussion

In this research, results of calculated indices have been compared with extracted lineaments and geology map of the study area.

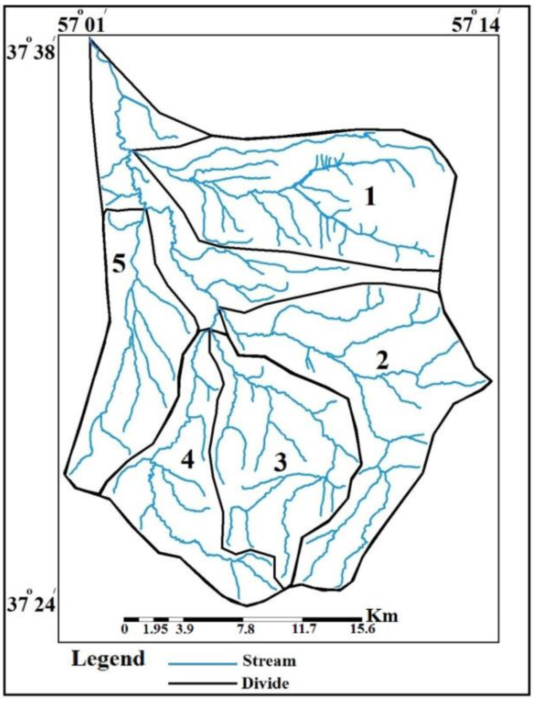

Figure 6) Subbasin's of Qharajeh basin and its reference number.

Relative tectonic activities were achieved by calculating geomorphic indices and averaging from them. Study area (Qharajeh basin) has 5 subbasins, subbasin 2 is largest subbasin and subbasin 4 is smallest subbasin (Fig. 6).

In this research for identifying more active and less active subbasin, geomorphic indices were calculated. Values of each index and *Iat* index is shown in Table 1.

Table 1) Classification of geomorphic index in Qharajeh basin.

Iat Class	S/n	Vf Class	Vf	SL Class	SL	Hi Class	Hi	Af Class	|Af–50|	Af	Sub basin
4	3	3	1.23	3	216	3	0.40	3	6	56	1
1	1.25	1	0.3	2	423	1	0.56	1	28	78	2
1	1	1	0.4	1	675	1	0.58	1	30	80	3
2	1.5	2	0.7	1	625	1	0.72	2	9	59	4
3	2.25	3	1.12	3	281	2	0.53	1	16	76	5

In Qharajeh basin *Af* varies from 56 (subbasin 1) to 80 (subbasin 3), the highest values of *Af* index demonstrate the most prominent asymmetry occurred in subbasin 2 and 3 (Fig. 7).

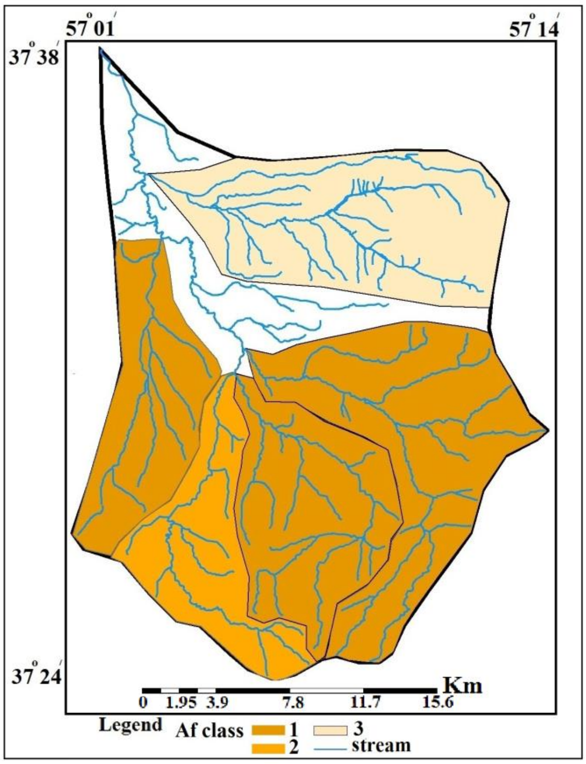

Figure 7) Distribution of Af index in study area.

This two subbasin (subbasins 2 and 3) were tilted to the border middle them. Calculated *Af* index shows that, increasing *Af* index in 2 and 3 subbasins is associated with high resistance lithology of this area and high rate of uplifting at this two subbasins.

Highest values of *Af* index in subbasin 2 and 3 is related to accumulation of lineaments in this area. In subbasin 1 value of *Af* index is close to 50, in this subbasin there is little tilting perpendicular to the direction of the master stream. Lowest amount of *Af* index in subbasin 1 is related to accumulation of alluvial deposits and low concentration of lineament in this subbasin.

Highest value of *T* index is related to southern subbasin it seems that folds and trusts parallel to this subbasin caused such tilting. Calculating morphometric indices for Qharajeh basin's show that, value of *T* index is 0.25. In southern subbasin some of rivers migration direction is toward East and West, existing fold in the south side of study area caused river tilting perpendicular to folds direction toward East and West (Fig. 8).

Calculating hypsometric curve is a powerful tool for differentiating tectonically active from inactive areas. Computed hypsometric curve shows that subbasin 1 is more active part of mainbasin and subbasin 4 is low active part of mainbasin (Fig. 9). *Hi* index computed for each subbasin, ranges from 216 (Subbasin 1) to 0.72 (Subbasin 4). Computing of hypsometric integral (*Hi*) shows that actives part of Qharajeh basin is south part of Qharajeh basin (subbasins 2, 3, 4) (Fig. 10).

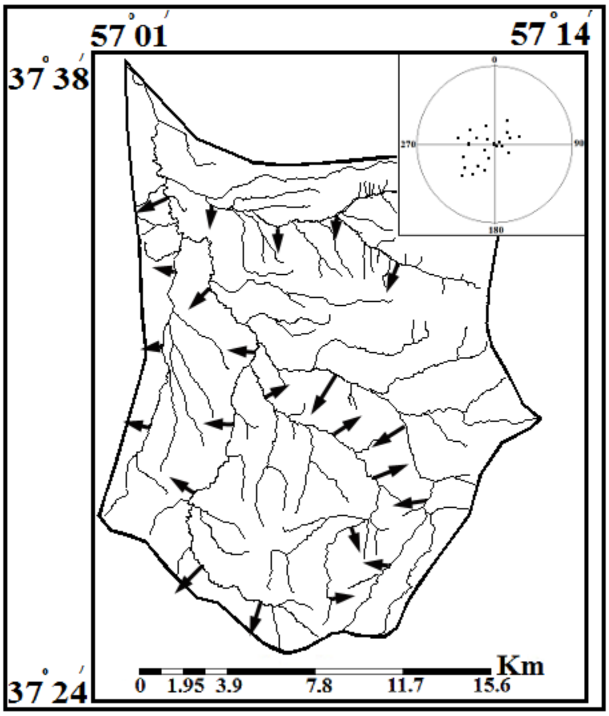

Figure 8) Transverse topographic symmetry factor for the study area and polar plot diagram of asymmetry vectors, at center magnitude =0; at margin magnitude =1.

Calculating hypsometric integral shows that in southern side of main basin (subbasins 2, 3, 4), rate of uplift are faster than rate of erosion. Value of *Hi* index in subbasin 5 is lower than mentioned subbasins, decrease of hypsometric integral in this subbasin is related to lithology and lowest concentration of lineament in this sub basin.

The lowest value of hypsometric integral (*Hi*) is related to north side of main basin and subbasin 1. subbasin 1 is Inactive, low amount of *Hi* index in this subbasin is associated with high erosion able rock of this subbasin. Existing alluvial deposits with low resistant at this area cause that rate of erosion be more than rate of uplift in this subbasin.

SL index were calculated along river using topographic map (1:25000) in GIS, value of SL index for each subbasin computed by averaging. It ranges from 0.40 (Subbasin 1) to 675 (Subbasin 3). Lowest amount of SL index is related to northern subbasins, highest amount of

SL index is related to southern subbasins (Fig. 11). Increasing SL index to southern subbasins is related to concentration lineament and rivers offset in this subbasins. Longitude river profile derived from DEM shows that upstream of all basins is inactive (Fig. 12).

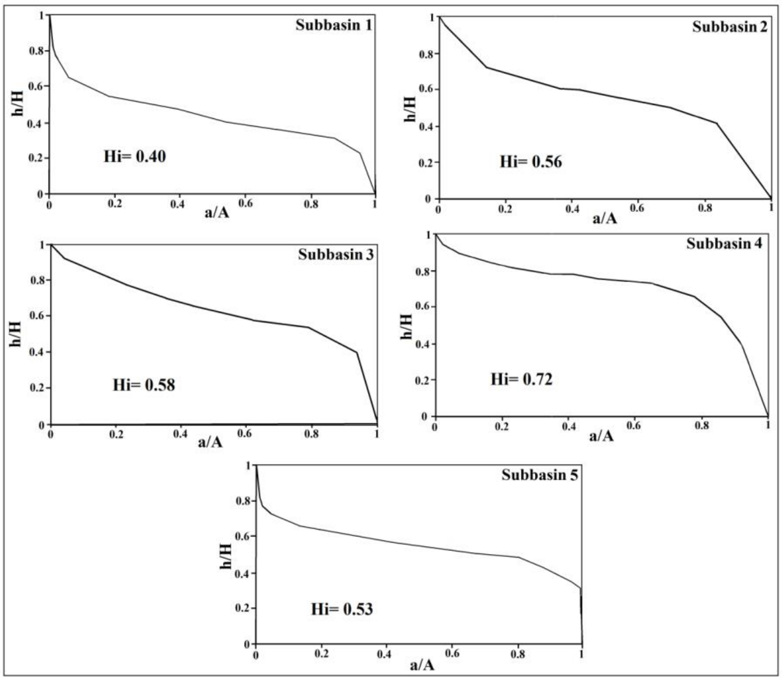

Figure 9) Hypsometry curves of subbasins of the Qharajeh basin. (A) is the total surface of the basin. (a) is the surface area within the basin above a given line of elevation (h), (H) is the highest elevation of the basin.

Longitude river profile of subbasins 2 indicate that except upstream, tectonic activity in other side of stream is moderate.

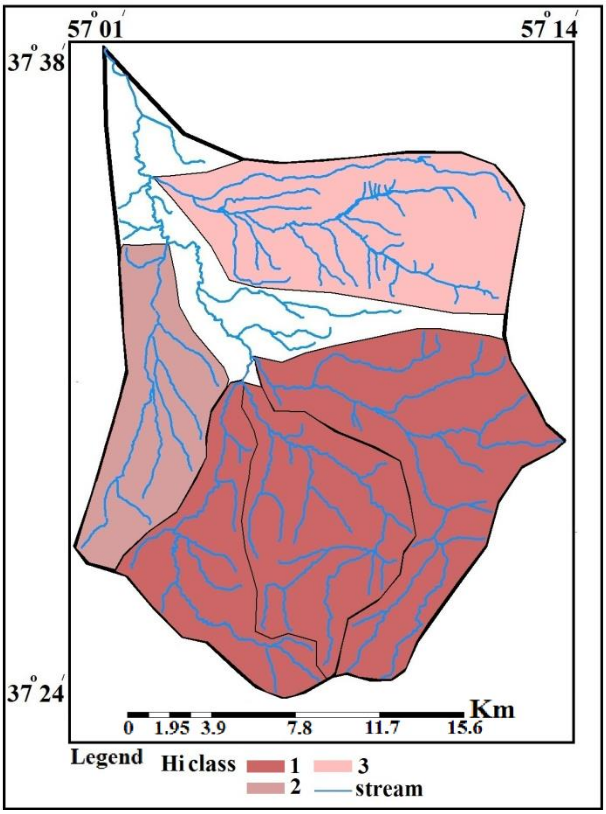

Figure 10) Distribution anomalies of Hi index in Qharajeh basin.

Derived profile from DEM for 3 and 4 subbasins show that upstream is inactive, tectonic activity in middle side of this tow subbasins is moderate and tectonic activity in downstream is high. Derived profile for main stream indicates that upstream and downstream is inactive and middle side of main basin is active part of Qharajeh basin.

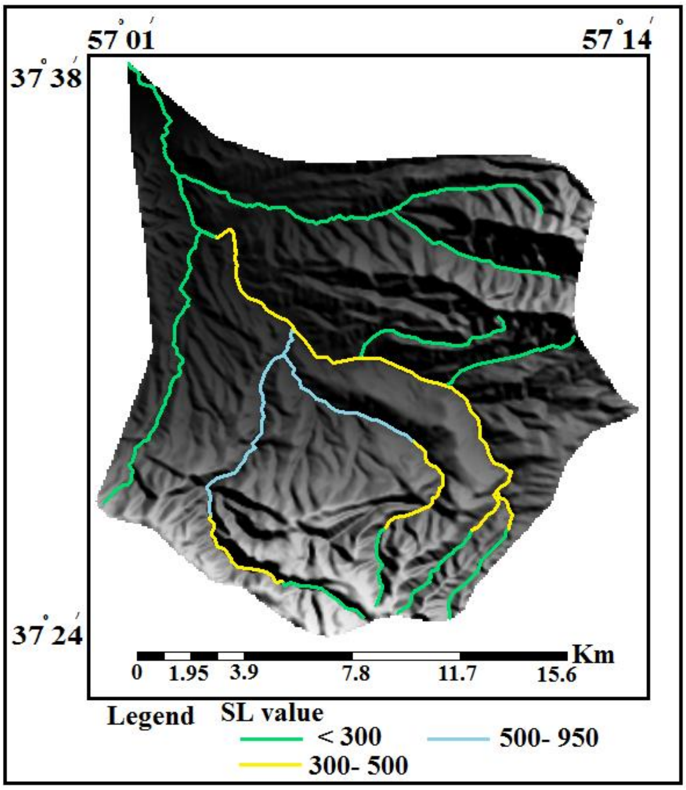

Figure 11) Distribution SL index along drainage b asin's river.

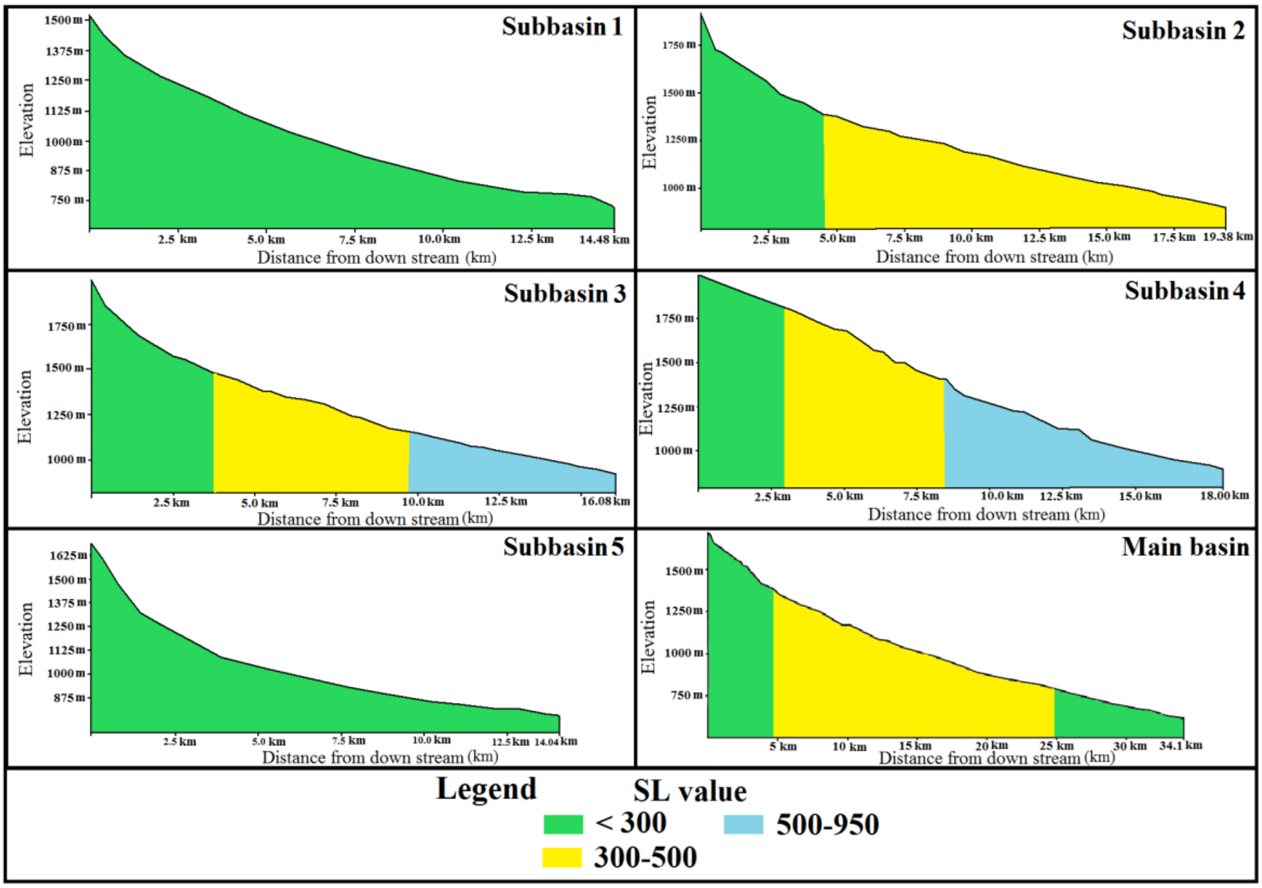

Figure 12) Longitudinal profile of river, derived from DEM and showing relationship between the slope and SL index values.

In this research for calculation *Vf* index digital elevation model (DEM) was utilized. *Vf* index ranges from 0.3 (Subbasin 2) to 1.23 (Subbasin 1).

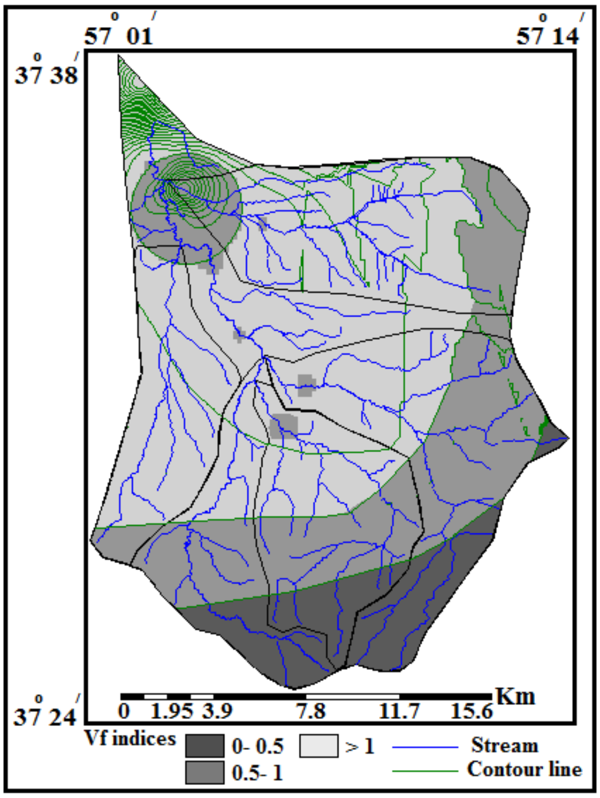

Figure 13) Ratio of valley floor width to valley height (Vf) for the study area.

Lowest values are associated with southern subbasin and highest values are associated with northern subbasin (Fig. 13). Computing of *Vf* index shows that high value of *Vf* index, low uplift rate and *U* shape valleys (broad– floor canyon) are associated with northern subbasins; and low value of Vf index, high uplift rate and *V* shape valleys are associated with southern subbasins (Fig. 14). Decreasing of *Vf* index in northern subbasin is associated with accumulation of high erosion able rocks and low rate of uplift in this part of basin.

The highest class values for *Iat* mainly occur in the north of Qharajeh basin, while the rest of study area has classes of *Iat* suggesting moderate to high tectonic activity. The distribution of indices defines areas associated with different rates of tectonic activity. Within the study area 2 subbasin (subbasin 2 and 3) is about class 1 (very high relative tectonic activity), subbasin 4 is about class 2 (high relative tectonic activity), subbasin 4 is about class 3 (moderate values of tectonic activity), subbasin 1 is about class 4 (lowest values of relative tectonic activity) (Fig. 15).

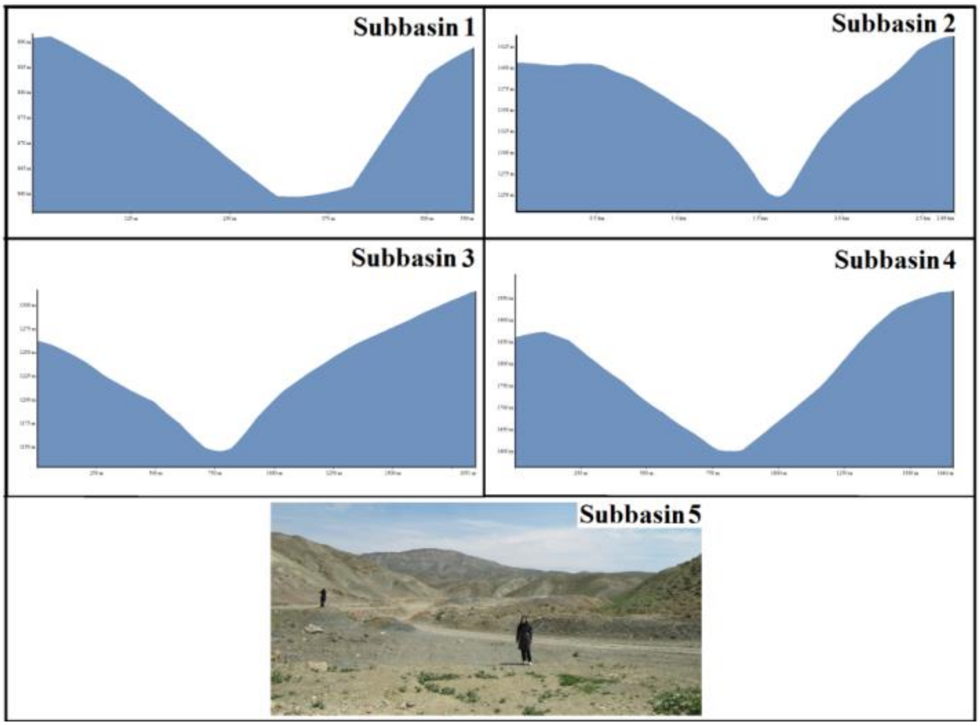

Figure 14) Shape of subbasins valley derived from DEM, and field survey.

Result of this study shows that in subbasins with high rate of uplifting *Iat* values is decreased and in areas with low rate of uplift *Iat* values is increased. Comparing Iat index with geology map of Qharajeh basin shows that in each subbasin alluvial deposits has higher concentration *Iat* index have highest value.

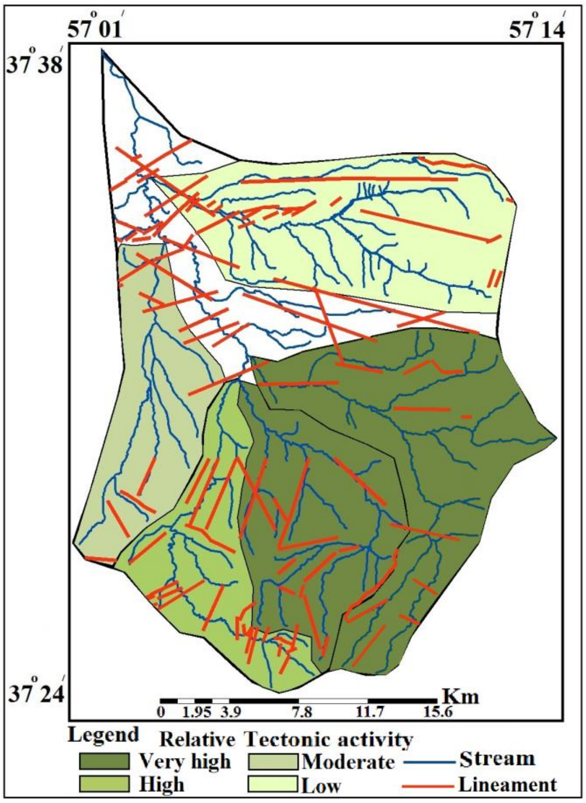

Figure 15) Distribution of the Iat index of Relative tectonic activity in Qharajeh basin

5– Conclusions

Geomorphic indices can be estimated for identify active part of each basin and determining level of tectonic activity in each area. In this research for separating high tectonic activity areas from low tectonic activity areas geomorphic indices such as drainage basin asymmetry factor (*Af*), transverse topographic symmetry factor (*T*), hypsometric integral (*Hi*) hypsometric curve (*Hc*), stream–gradient index (*SL*), valley floor width–valley height ratio (*Vf*) and combination of all indices (*Iat*) were calculated. Highest amount of *Af* and T indices is associated with southern subbasin, the values of *Af* and *T* indices is related to tectonic tilting. Calculating these tow indices shows that highest tilting is associated with southern subbasin. Value of *Hi* index were found to be high in southern subbasin, Computing of *Hi* index shows that rate of uplifting in southern subbasins is more than other subbasins. Calculating *SL* index showed that, high tectonic activity of study area is related to southern subbasins and offset of streams in this area. values of *Vf* index showed that most southern subbasin is narrow and deep, this index indicate that high rate of incision in southern subbasin is associated with tectonic uplift in this area. Relative tectonic activity (*Iat*) calculated by averaging from all indices. Class 1 of *Iat*, indicating that most active tectonics occurs in the southwestern part of the study area along high resistance rock and high accumulated lineament. Class 2 and 3 of *Iat* corresponding to highly and moderate active tectonics occurs in west of study area is associated with lower lineament accumulation than southern subbasin. Class 4 of *Iat* mainly takes place in the tectonically inactive anticline and plains in the northeastern parts of the study area.

Acknowledgments:

The authors would like to thank Dr. R. Raj and Dr. R. Alipoor for their kind and careful comments that made the manuscript improved.

References:

Adams, j. 1980. Contemporary uplift and erosion of the Southern Alps. New Zealand: Geological Society of America Bulletin: 91, 1–114.

Alavi, M. 1991. Sedimentary and Structural characteristics of the Paleo–Tethys remnants in northeastern Iran. Geological Society of America Bulletin: 103, 983–992.

Alavi, M. 1996. Tectonostratigraphic synthesis and structural style of the Alborz mountain system in northern Iran. Journal of Geodynamics: 21, 1–33.

Arisco, G., Arnone, G., Favara, R., Nigro, F., Perricone, M., Renda, P., Mondello, C. 2006. Integrated neotectonic and morphometric analysis of northern Sicily.

Bollettino della society Geological Italiana: 125, 129–153.

Berberian, M., and King, G. 1981. Towards a palaeogeography and tectonic evolution of Iran. Canadian Journal of Earth Science: 18, 210–265.

Cox, R.T. 1994. Analysis of the drainage basin symmetry as a rapid technique to identify areas of possible quaternary tilt–block tectonics: an example from the Mississippi Embayment. Geological Society of America Bulletin: 106, 571–581.

Cox, R.T., Van Arsdale, R. B., and Harris, J. B. 2001. Identification of possible Quaternary deformation in the northern Mississippi embayment using quantitative geomorphic analysis of drainage–basin asymmetry. Geological Society of America Bulletin: 113, 615–624.

Dehbozorgi, M., Pourkermani, M., Arian, M., Matkan, A. A., Motamedi, H., Hosseiniasl, A. 2010. Quantitative analysis of relative tectonic activity in the Sarvestan area, central Zagros, Iran. Geomorphology: 121, 329–341.

EL Hamdouni, R., Irigaray, C., Fernandez, T., Chacon, J., and Keller, E.A. 2008. Assessment of relative active tectonics, southwest border of Sierra Nevada (southern spain). Geomorphology: 969, 150–173.

Hack, J.T. 1973. Stream– profile analysis and stream–gradient index. Geological Survey Journal of Research: 1, 421–429.

Hollingsworth, J. 2007. Active tectonics of NE Iran. Ph.D Thesis, University of Cambridge, p 239.

Hollingsworth, J., Fattahi, M., Walker, R., Talebian, M., Bahroudi, A., Bolorchi, M.J., Jackson, J., Copley, A. 2010. Oroclinal bending, distributed thrust and strike–slip faulting, and the accommodation of Arabia–Eurasia convergence in NE Iran since the Oligocene. Geophysical Journal International: 181, 1214-1246.

Jackson, J., and Mc Kenzie, D. 1984. Active tectonics of the Alpine–Himalayan Belt between Turkey and Pakistan. Geophysical Journal of the Royal Astronomical Society: 77, 185–264.

Keller, E.A., and Pinter, N. 1996. Active tectonic, Earthquickes, Uplift and Landscape. Prentice Hall, P. 362.

Keller, E.A., and Pinter, N. 2002. Active tectonic, Earthquickes, Uplift and Landscape. Prentice Hall P. 362.

Khavari, R., Arian, M. 2010. Active Tectonics of the South Central Alborz (North Iran). Australian Journal of Basic and Applied Sciences: 4, 969–963.

Pike, R.J., and Wilson, S.E. 1971. Elevation relief ratio, hypsometrynintegral and geomorphic area–altitude analysis. Geological Society of America Bulletin: 62, 1079–1084.

Ribolini, A., Spagnolo, M. 2008. Drainage network geometry versus tectonics in the Argentera Massif (French–Italian Alps). Geomorphology: 93, 253–266.

Slemmons, D.B., Slemmons, D.B., Engdahl, E.R., Zoback, M.D., Blackwell, D.D. (eds.). 1991. Neotectonics of North America. Geological Society of America: 1–20.

Stepancikova, P., Stemberk, J., Vilimek, V., Kostak, B. 2008. Neotectonic development of drainage networks in the East Sudeten Mountains and monitoring of recent fault displacements (Czech Republic). Geomorphology: 102, 68–80.

Stocklin, J. 1968. Structural history and tectonics of Iran: A review. American Association of Petroleum Geology Bulletine, 52, 1229–1258.

Verrios, S., Zygouri, V., Kokkalas, S. 2004. Morphotectonic analysis in the Eliki fault zone (Gulf of Corinth, Greece). Bulletin of the Geological Society of Greece: 36, 1706–1714.